

## C-2U: A Sustained Neutral Beam Driven Field-Reversed Configuration

L. Schmitz,<sup>1,2</sup> M.W. Binderbauer,<sup>1</sup> H. Gota,<sup>1</sup> T. Tajima,<sup>1,3</sup> C. Lau,<sup>3</sup> D. Fulton,<sup>1</sup> Z. Lin,<sup>3</sup> B.H. Deng,<sup>1</sup> S. Putvinski,<sup>1</sup> M. Tuszewski,<sup>1</sup> S. Detrick,<sup>1</sup> E. Garate,<sup>1</sup> S. Korepanov,<sup>1</sup> A. Smirnov,<sup>1</sup> M.C. Thompson,<sup>1</sup> and the TAE Team

<sup>1</sup>Tri Alpha Energy, Inc., Rancho Santa Margarita, CA 92688, USA

<sup>2</sup>University of California Los Angeles, Los Angeles, CA 90095-7799, USA

<sup>3</sup>University of California Irvine, Irvine, CA 92697, USA

Sustained Field-Reversed Configuration (FRC [1,2]) plasmas have recently been achieved in the upgraded C-2U device [3], the world's largest compact toroid (CT) device ( $T_i \leq 1$  keV,  $T_e \leq 0.15$  keV,  $\langle n \rangle \leq 4 \times 10^{19} \text{ m}^{-3}$ ). Crucial ingredients for FRC sustainment are (i) increased total neutral beam injection (NBI) input power  $\geq 10$  MW (15 keV hydrogen) with tilted injection angle; (ii) enhanced edge-biasing capability for stability control via coaxial plasma guns located in the C-2U divertor sections. In the best operating regime we have successfully achieved plasma sustainment times up to  $t_s \geq 5$  ms, via building up NBI-supported, well-confined fast particle populations. In the longer-pulse regime the plasma lifetime can be extended up to and beyond the end of the NBI pulse-duration ( $t_s \geq 8$  ms). In the FRC core, ion-scale turbulence is absent, and only weak electron-scale modes have been detected ( $0.04 \leq k_\phi \rho_e \leq 0.4$ ,  $5 \leq k_\phi \rho_s \leq 50$ , where  $\rho_e, \rho_s$  are the electron gyroradius and the ion sound gyroradius). In addition to controlling macroscopic (toroidal mode number  $n=1,2$ ) MHD-modes, edge biasing produces radially sheared  $\mathbf{E} \times \mathbf{B}$  flow at/outside the FRC separatrix, substantially reducing scrape-off layer (SOL) density fluctuations measured via multichannel Doppler Backscattering (DBS), and dramatically improving particle and energy confinement.

Figure 1 shows the normalized excluded flux radius (measured via plasma diamagnetism) for a sequence of FRC discharges obtained at different times as C-2 and C-2U capabilities and performance were upgraded. A detailed description of the C-2 and C-2U geometry and

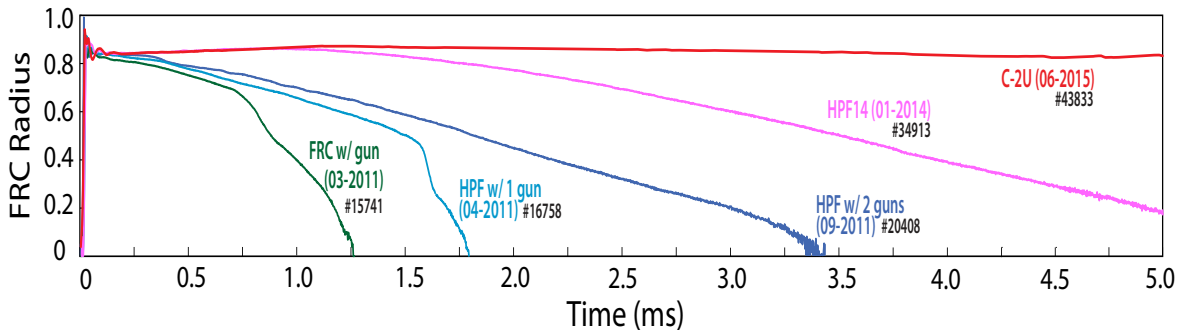


Fig. 1: Time evolution of FRC midplane normalized excluded flux radius: FRC with gun (biased) (C-2); FRC supported via one axial plasma gun and NBI ( $\sim 4$  MW) (C-2); FRC supported with two plasma guns and NBI ( $\sim 4$  MW, High Performance FRC (HPF) regime C-2); FRC supported via plasma guns and high power NBI (10 MW) in C-2U.

experimental setup can be found in [3,4]. The application of negative electrostatic biasing of the SOL plasma via 1-2 plasma guns (PGs [5-7]) placed in the divertor sections (at a distance of  $\pm 8.8$  m from the machine midplane), and the application of Neutral Beam Heating (NBI) with  $P_{\text{NBI}} \sim 4$  MW) resulted in greatly improved FRC stability with respect to tilt modes and  $n=2$  rotational modes, and substantially increased life times. Increased performance (indicated as HPF14 regime) has been achieved with increased magnetic field in the plasma formation sections. A further dramatic improvement with  $t_s \geq 8$  ms has been achieved in C-2U, using two plasma guns along with upgraded NBI power ( $P_{\text{NBI}} \sim 10$  MW) as indicated in Fig.1.

Figure 2 shows the concomitant improvement in global FRC energy confinement, obtained via power balance analysis over a time period 1.5-3 ms (0.5-1ms and 0.5-1.5ms, respectively, in the bias-only and one gun/NBI-supported cases). Compared to an unbiased FRC, energy confinement is improving substantially with bias and NBI. A more significant improvement is achieved with two PGs and NBI in the HPF-14 (High Performance FRC) configuration, where the axial magnetic field in the FRC formation sections was increased to improve contact of the SOL plasma with the biased plasma guns.

Figure 3 shows the turbulence wavenumber spectrum measured in the confined FRC core (at  $r/R_s=0.75-0.85$ , where  $R_s$  is the separatrix flux radius), and in the SOL (at  $r/R_s=1.15-1.2$ ), vs. toroidal turbulence wavenumber. The fluctuation data reported here is acquired via Doppler Backscattering (DBS [8,9]). DBS simultaneously measures the density fluctuation level at a specific toroidal wavenumber for different plasma radii, both in the FRC core and in the SOL. Collinear Gaussian beams are launched into the plasma at an oblique angle  $\zeta$  in the toroidal plane, as described in more detail elsewhere [9]. Backscattering by plasma density fluctuations occurs preferentially near the plasma cut-off layer for each launched frequency. The probed radial wavenumber is  $k_r \sim 0$  as the beams propagate toroidally near the plasma cut-off layer. The wavenumber  $k_\theta$ , and the probed radii  $r$  in the laboratory frame are calculated using GENRAY [10] ray tracing based on high time resolution (10  $\mu$ s) radial electron density profiles reconstructed from a six channel CO<sub>2</sub> laser interferometer [11]. The rms density fluctuation level ( $0.5 \leq k_\theta \rho_s \leq 40$ ), toroidal  $\mathbf{E} \times \mathbf{B}$  velocity, and decorrelation rate near the FRC midplane are evaluated from the amplitude and Doppler shift of the

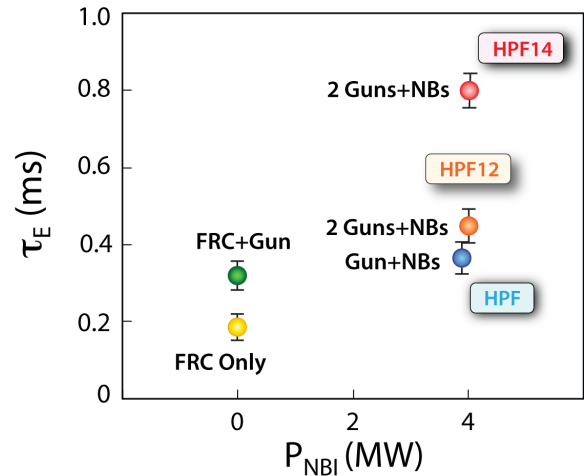


Fig. 2: Global FRC energy confinement time from power balance for a simple FRC; FRC with plasma gun (PG); FRC supported by one/two PGs and NBI, and for an FRC supported via NBI and 2 PGs in the HPF14 configuration with increased formation magnetic field.

backscattered signals. An inverted toroidal wavenumber spectrum is measured in the closed flux surface FRC core region, indicating clearly that ion-scale turbulence is substantially reduced. Near-classical ion thermal energy confinement ( $\chi_i \sim (1-2)\chi_i^{cl}$ ) is inferred from 1-D power balance analysis [12], in qualitative agreement with the absence of large-scale core turbulence. In contrast, an exponential wave-number spectrum is observed in the SOL, extending from  $k_\theta \rho_s > 3$  well into the electron mode range,  $k_\theta \rho_e \leq 0.5$ ). Linear, local

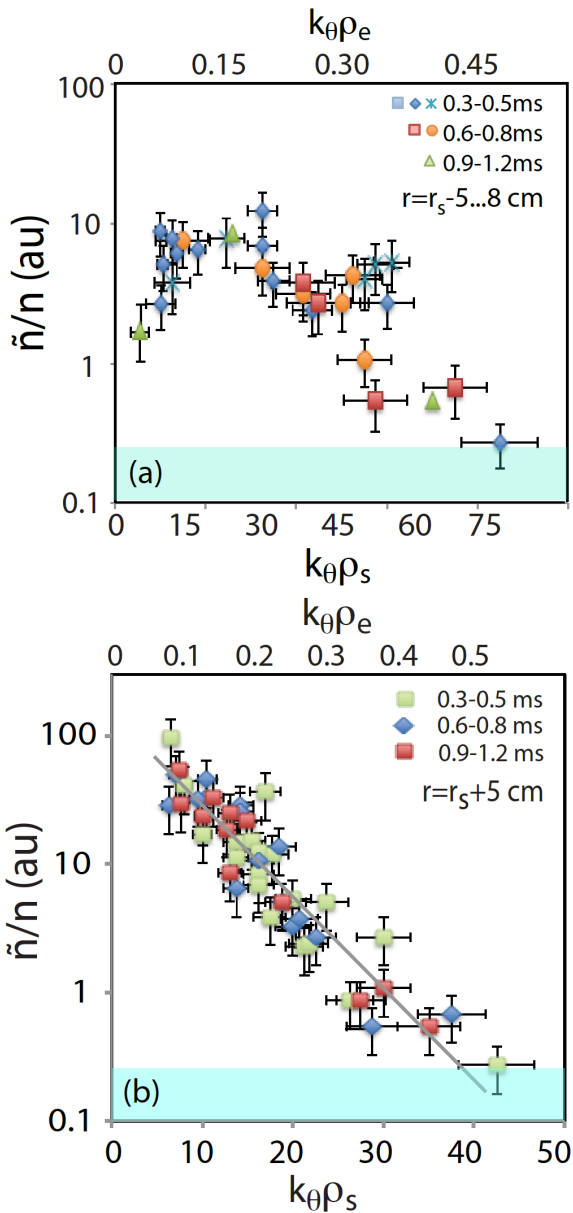


Fig. 3 Toroidal wavenumber spectrum of density fluctuations, measured via DBS. (a) Density fluctuation level vs. normalized toroidal wavenumbers  $k_\theta \rho_e$  and  $k_\theta \rho_s$  in the FRC core inside the separatrix, and (b) and in the SOL (shots #29587-29610; #29750-29802). The DBS sensitivity limit is indicated (blue-green bar).

(flux-tube) electrostatic gyrokinetic simulations, using a modified version of the GTC code [13-15] confirm that ion modes are stable in the FRC core. No unstable modes (either drift waves with  $k_{\parallel} \neq 0$  or interchange modes with  $k_{\parallel} = 0$ ) have been found for realistic values of the normalized radial density gradient ( $R/L_n < 6$ ) and realistic values of the normalized electron and ion temperature gradients [16]. The FRC core simulations suggest that lower- $k$  modes are absent due a combination of Finite Larmor radius effects [17-19], the short field line connection length in the (closed flux surface) FRC core, and the magnetic field gradient which increases with radius. In contrast, simulations for the FRC SOL indicate unstable drift-interchange modes for  $k_\theta \rho_s > 1.5$ , with lower wavenumbers still mitigated/stable primarily via FLR effects. The measured density fluctuations near the separatrix and in the SOL exhibit a critical density gradient (normalized by the null-field radius  $R$ ) [Figure 4(a-c)] roughly in agreement with the linear instability threshold calculated from GTC [Fig. 4(d)]. A lower linear threshold is calculated for high toroidal wavenumber, however the energy density in the higher- $k$  part of the spectrum is substantially lower, and the associated radial transport rates are expected to be lower. A moderately large SOL critical gradient, as

measured here, is favorable for achieving a narrow SOL for reactor-like FRC parameters, leading potentially to a compact fusion core. The increased parallel heat flux in a narrow SOL can be exhausted in an axisymmetric FRC via radial magnetic flux expansion.

In conclusion we have presented strong evidence from experimentally measured wavenumber spectra and gyrokinetic simulations that large-scale, ion-range modes are stable in the C-2/C-2U FRC core. This result, qualitatively in agreement with transport analysis in C-2, is highly promising for FRC confinement. Further work is needed to incorporate SOL/FRC core coupling into the gyrokinetic simulations, as well as to perform nonlinear runs including electromagnetic effects.

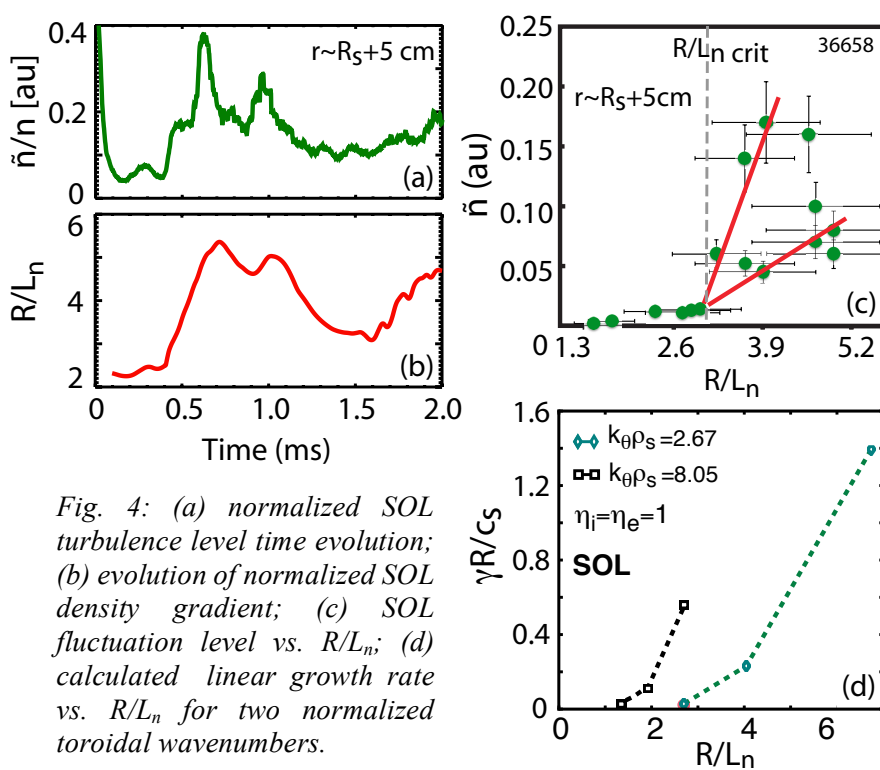


Fig. 4: (a) normalized SOL turbulence level time evolution; (b) evolution of normalized SOL density gradient; (c) SOL fluctuation level vs.  $R/L_n$ ; (d) calculated linear growth rate vs.  $R/L_n$  for two normalized toroidal wavenumbers.

1. M. Tuszewski, *Nucl. Fusion* **28**, 2033-3093 (1988).
2. L.C. Steinhauer, *Phys. Plasmas* **18**, 070501 (2011).
3. M. Binderbauer et al. *Phys. Plasmas* **22**, 056110 (2015).
4. M. Binderbauer, et al. *Phys. Rev. Lett.* **105**, 045003 (2010).
5. T.D. Akhmetov et al. *Fusion Sci. Technology* **43**, 58-62 (2003).
6. M. Tuszewski, A. Smirnov, M.C. Thompson, et al. *Phys. Plasmas* **19**, 056108 (2012).
7. M. Tuszewski, M. et al. *Phys. Rev. Lett.* **108**, 255008 (2012).
8. C. Hillesheim, W. A. Peebles, T. L. Rhodes, L. Schmitz, A. E. White, and T. A. Carter, *Rev. Sci. Instrum.* **81**, 10D907 (2010).
9. L. Schmitz, L. et al. *Rev. Sci. Instrum.* **85**, 11D840 (2014).
10. A.P. Smirnov and R.W. Harvey, The GENRAY ray tracing code, *CompX Report COMPX-2000-01* (2001).
11. B.H. Deng, J.S. Kinley, and J. Schroeder *Rev. Sci. Instr.* **83**, 10E339 (2012).
12. S. Gupta S., D.C. Barnes, S.A. Detrick, E. Trask et al. *Phys. Plasmas* **23**, 052307 (2016).
13. Z. Lin, T.K Hahm, et al. *JPSJ* **281**, 1835-1837 (1998).
14. D. P. Fulton, C.K. Lau, I. Holod, Z. Lin, S.A. Detrick et al. *Phys. Plasmas* **23**, 012509 (2016).
15. D. P. Fulton, C.K. Lau, L. Schmitz, I. Holod, Z. Lin et al. *Phys. Plasmas* **23**, 056111 (2016).
16. L. Schmitz et al., submitted to *Nature Communications*.
17. H. Naitou, H., T. Kamimura, and J.M. Dawson *JPSJ* **46**, 258-265 (1979).
18. M.N. Rosenbluth, N. Krall, and N. Rostoker, *Nucl. Fusion Supplement Pt. 1* 143-150 (1962).
19. N. Rostoker, in "Physics of High Energy Particles in Toroidal Systems" Editors T. Tajima and M. Okamoto (American Institute of Physics, New York, 1994), pp.323.